STANFORD RESEARCH INSTITUTE

MENLO PARK, CALIFORNIA

March 1967

Technical Report 1

RESONANCES IN THE DRIVING-POINT IMPEDANCE OF AN ELECTRIC DIPOLE IN THE IONOSPHERE

By: W. E. BLAIR

Prepared for:

STANFORD UNIVERSITY
STANFORD, CALIFORNIA

SUBCONTRACT RA-0023 UNDER
CONTRACT NAS5-9309

SRI Project 6045

Approved: W. R. VINCENT, MANAGER
COMMUNICATION LABORATORY

D. R. SCHEUCH, EXECUTIVE DIRECTOR
ELECTRONICS AND RADIO SCIENCES

Copy No. 28

ABSTRACT

The resonances in the driving-point impedance of a center-fed cylindrical electric dipole imbedded in the ionosphere are analyzed. The ionospheric model is a lossy, anisotropic, homogeneous neutral plasma containing various ionic constituents. It is found that there are zeros in the reactance at the upper and lower hybrid frequencies and poles at the electron and ion gyrofrequencies. These critical frequencies are independent of antenna length and orientation (parallel or perpendicular to the earth's magnetic field) to the first-order approximation. It is shown that pole-zero frequencies could be used to determine the earth's magnetic field strength, electron density, and ion masses and densities at any point in the ionosphere at which the impedance was measured.

CONTENTS

ILLUSTRATIONS

GLOSSARY OF SYMBOLS

a = antenna radius.

A^2 = $(r_0^2/4)W^2/(1 + r_0^2/4) = (r_0^2/4)U^2$.

B = $(1 + r_0^2/4)^{-1/2}$.

B_0 = the earth's magnetic field, assumed to be uniform in the vicinity of the antenna.

C^2 = $r_0^2 W^2/(1 + r_0^2) = r_0^2 V^2$.

D = $(1 + r_0^2)^{-1/2}$.

f = the signal frequency.

I_0 = the source current magnitude.

K^2 = $(\kappa_{11}/\kappa_{33})$.

k_a = the propagation wave number along the antenna.

l = the antenna half-length.

L = McIllwain L parameter.

m_n = the particle mass.

N_n = the particle density.

q_n = the particle charge.

$$r = \frac{a}{l}\left(\frac{\kappa_{11}}{\kappa_{33}}\right)^{-1/2}.$$

r_0 = a/l.

R = the distance from the center of the earth to the point of observation.

R_E = the earth's radius.

U = WB.

U_n = $1 - jZ_n$.

V = WD.

$W = K^2 - 1.$

$X_n = \dfrac{N_n q_n^2}{\omega^2 m_n \epsilon_0} = \dfrac{\omega_{pn}^2}{\omega^2}.$

$Y_n = \dfrac{B_0 q_n}{\omega m_n} = \dfrac{\omega_{gn}}{\omega}.$

z = the direction along the antenna, whose source is positioned at $z = 0$.

$Z_{dp}^{\parallel}$ = the driving-point impedance for an antenna oriented parallel to B_o.

$Z_{dp}^{\perp}$ = the driving-point impedance for an antenna oriented perpendicular to B_o.

$Z_n = \dfrac{\nu_n}{\omega}.$

ϵ_0 = the permittivity of free space.

$\kappa_{11} = 1 - \sum_n \dfrac{X_n U_n}{U_n^2 - Y_N^2} = (\mu_R^2 + \mu_L^2)/2.$

$\kappa_{12} = \dfrac{X_n Y_n}{U_n^2 - Y_n^2} = (\mu_R^2 - \mu_L^2)/2.$

$\kappa_{33} = 1 - \sum_n \dfrac{X_n}{U_n} = \mu_0^2.$

μ_L = the refractive index of a left circularly polarized mode.

μ_0 = the refractive index of the ordinary mode.

μ_R = the refractive index of the right circularly polarized mode.

μ_X = the refractive index of the extraordinary mode.

ν_n = the collision frequency.

$\omega (= 2\pi f)$ = the radian frequency.

ω_{gn} = the gyroresonance radian frequency.

ω_{pn} = the plasma resonance radian frequency.

ACKNOWLEDGMENTS

The author is grateful to N. M. Brice of Cornell University, R. L. Smith of Stanford University, and S. V. Yadavalli of the Mathematical Physics Department of Stanford Research Institute for fruitful discussions and to A. R. Geoffrion for computer programming.

1 INTRODUCTION

An electric antenna imbedded in a magnetoplasma, such as the ionosphere, interacts strongly with the medium at certain critical frequencies. Basically, an electric antenna couples strongly to a medium whose relative permittivity is much larger than one (electric medium) and weakly to a medium whose relative permeability is much larger than one (magnetic medium). Thus the permittivity of an electric medium is more important than is the permeability to the interaction of an electric antenna with the medium. These previous two statements apply to a magnetic antenna if throughout the words electric and magnetic are interchanged and permittivity and permeability are interchanged.

The coupling of an antenna to the adjacent medium is observed directly through the measurement of the driving-point impedance. The driving-point impedance of an electric antenna in the ionosphere is sensitive in the first order to the characteristics of the permittivity, which is a complex function of frequency, mass, and density of the ionized constituents, the particle collisions, and the earth's magnetic field. On the other hand, the driving-point impedance of a magnetic antenna in the ionosphere is sensitive in the first order to the characteristics of the permeability,[1*] which is essentially that of free space.

Several approaches have been used to calculate the various effects of the ionosphere on the driving-point impedance of a dipole imbedded in the ionosphere. A quasi-static approximate solution has been used by Blair[2,3] and a quasi-static mathematical model has been used by Balmain.[4] These two formulations, yielding essentially the same results, are the bases for the work in this paper. The impedance at the upper (electron) hybrid resonance and the electron plasma resonance have been studied both theoretically[5] and experimentally.[6] The lower hybrid resonance has been discussed by Fejer for pulse responses.[7]

---

* References are listed at the end of the report.

Other models have used a sinusoidal current distribution,[1,8] thus requiring the correct propagation constant on the antenna.[9] Here an electrically-short antenna is used, so that antenna propagation constant is not needed in the analysis. There are no possible infinities in the resistance, since an antenna of finite radius and length is used.[10] A "cool" ionospheric model is used, and only losses (collisions) are considered. Other temperature effects,[11] including kinetic theory effects,[12,13] have not been considered. However, the hot plasma compressibility effects[14] have not been considered. The ionosphere is assumed to be homogeneous with no sheath resonances[15,16] considered in the analysis. A comprehensive set of references on this subject is given by Galejs.[15]

The Stanford University/Stanford Research Institute VLF experiments aboard OGO-III and two future OGO satellites are designed in part to measure the driving-point impedance of an electric antenna. The theoretical work herein will be compared with the experimental data from these experiments to determine the validity of the assumptions of this model.

2. MODELS AND FORMULAS

2.1 Driving-Point Impedance Formulas

The driving-point impedance ($Z^{\parallel}_{dp}$) of a center-fed, cylindrical, electrically short dipole oriented parallel to the earth's magnetic field and imbedded in a homogeneous, lossy magnetoplasma is:[2,3,4]

$$Z^{\parallel}_{dp} = \frac{-j}{\pi\omega\epsilon_0\kappa_{11}l}\left(ln\left\{\frac{1}{2r}\,\frac{[1 + (1 + r^2)^{1/2}]^2}{[1 + (1 + r^2/4)^{1/2}]}\right\} - 2(1 + r^2)^{1/2} + (1 + r^2/4)^{1/2} + (3/2)r\right) , \tag{1}$$

where $2l$ is the antenna length and κ_{11} is the diagonal element of the permittivity tensor, κ, describing the Appleton-Hartree magnetoionic model of the ionosphere:[17]

$$\overset{\wedge}{\kappa} = \begin{bmatrix} \kappa_{11} & j\kappa_{12} & 0 \\ -j\kappa_{12} & \kappa_{11} & 0 \\ 0 & 0 & \kappa_{33} \end{bmatrix} , \tag{2}$$

and where

$$\kappa_{11} = 1 - \sum_n \frac{X_n U_n}{U_n^2 - Y_n^2} = (\mu_R^2 + \mu_L^2)/2 \tag{3a}$$

$$\kappa_{12} = \sum_n \frac{X_n Y_n}{U_n^2 - Y_n^2} = (\mu_R^2 - \mu_L^2)/2 \tag{3b}$$

$$\kappa_{33} = 1 - \sum_n \frac{X_n}{U_n} = \mu_0^2 \tag{3c}$$

$$U_n = 1 - jZ_n \tag{3d}$$

$$X_n = \frac{N_n q_n^2}{\omega^2 m_n \epsilon_0} = \frac{\omega_{pn}^2}{\omega^2} \tag{4a}$$

$$Y_n = \frac{B_0 q_n}{\omega m_n} = \frac{\omega_{gn}}{\omega} \tag{4b}$$

$$Z_n = \frac{\nu_n}{\omega} \tag{4c}$$

N_n = particle density

q_n = particle charge

m_n = particle mass

B_0 = earth's magnetic field, assumed to be uniform in the vicinity of the antenna

ϵ_0 = permittivity of free space

ν_n = collision frequency

ω $(= 2\pi f)$ = radian frequency

f = signal frequency

ω_{pn} = plasma resonance radian frequency

ω_{gn} = gyroresonance radian frequency

$$r = \frac{a}{l}\left(\frac{\kappa_{11}}{\kappa_{33}}\right)^{-1/2}$$

l = antenna half length

a = antenna radius.

The subscript n indicates the n*th* constituent. Rationized MKS units are used throughout, and the harmonic time $e^{+j\omega t}$ is assumed. The elements, Eq. (3), of the permittivity matrix, Eq. (2), are also expressed in terms of the refractive indices, μ_r, μ_l for right-hand and left-hand polarized waves and μ_0, μ_X for ordinary and extraordinary waves.

Similarly, the driving-point impedance of a center-fed, cylindrical, electrically short dipole, oriented perpendicular to the earth's magnetic field and imbedded in a homogeneous, lossy magnetoplasma is:[3]

$$Z_{dp}^{\perp} = \frac{-j}{2\pi\omega\varepsilon_0(\kappa_{11}\kappa_{33})^{1/2}l}\left(\ln\left\{\frac{r_0^2}{2}\cdot\frac{(1+C)[1+(1-4W^2B^2)^{1/2}]}{(1+2B)[1-(1-W^2C^2)^{1/2}]}\right\} + I_1 + I_2 - \frac{2}{\pi}\frac{2}{C}\mathcal{E}\left[\frac{U}{(U^2+1)^{1/2}}\right] + \frac{2}{B}\mathcal{E}\left[\frac{V}{(V^2+1)^{1/2}}\right] - 3r_0\mathcal{E}(W)\right), \tag{5}$$

where

$$\begin{aligned} r_0 &= a/l \\ A^2 &= (r_0^2/4)W^2/(1+r_0^2/4) = (r_0^2/4)U^2 \\ B &= (1+r_0^2/4)^{-1/2} \\ C^2 &= r_0^2W^2/(1+r_0^2) = r_0^2V^2 \\ D &= (1+r_0^2)^{-1/2} \\ U &= WB \\ V &= WD \\ W &= K^2-1 \\ K^2 &= (\kappa_{11}/\kappa_{33}) \quad . \end{aligned} \tag{6}$$

Here $\mathcal{E}$ is the complete elliptic function of the second kind. The remainder integrals I_1 and I_2 are of order (r_0^2) such that

$$|I_1| \leq \left|\frac{\pi}{2} r_0^2\right| \quad , \quad r_0^2 << 1$$

$$|I_2| \leq \left|\frac{\pi}{2} \frac{r_0^2/4}{1 + r_0^2/4} (K^2 - 1)^2\right| \quad , \quad r_0^2 << 1 \quad . \qquad (7)$$

The electrically short dipole is assumed to have a triangular current distribution obtained from the following sinusoidal current distribution:

$$I(z) = I_0 \frac{\sin k_a(l - |z|)}{k_a l} \quad ,$$

where

I_0 = the source current magnitude

k_a = the propagation wave number along the antenna

z = the direction along the antenna, whose source is positioned at $z = 0$.

For $(k_a l) << 1$, then, the above current distribution is approximated by the following triangular current distribution:

$$I(z) \approx I_0(1 - |z|/l) \quad , \quad (k_a l) << 1 \quad .$$

It is fortunate that this quasi-static distribution does not contain the antenna wave number, k_a, since it is not well known and is a function of the plasma constituents and the earth's magnetic field.[9] In an ionosphere with typical collision losses, k_a can become large but finite depending on the antenna orientation (and the diameter of an ion sheath, if it exists); thus the constraint $(k_a l << 1)$ may require a very short antenna.[18]

2.2 Approximation of Driving-Point Impedance Formulas

The impedance formula given in Eq. (1) can be greatly simplified by using certain reasonable approximations. If the antenna is a typically long, thin cylindrical dipole and $r_0 << |(\kappa_{11}/\kappa_{33})^{1/2}|$, the following

approximate formula is useful for the antenna oriented parallel to the earth's magnetic field:

$$Z_{dp}^{\parallel} = \frac{-j}{\pi\omega\epsilon_0\kappa_{11}l}\left[ln(1/r) - 1\right] \quad , \quad |r| << 1 \quad . \tag{8}$$

For the conditions of the signal frequency near the natural resonances in the ionosphere, $\kappa_{11} \simeq 0$, and $r_0 >> |(\kappa_{11}/\kappa_{33})^{1/2}|$, Eq. (1) reduces to

$$Z_{dp}^{\parallel} = \frac{-j}{\pi\omega\epsilon_0\kappa_{11}l}\left(\frac{1}{4r^3}\right) \quad , \quad |r| >> 1 \quad . \tag{9}$$

Similarly, Eq. (5) can be simplified for the case of a typically long, thin cylindrical dipole and for the case of f less than the HF band and $f \neq f_p$. Then the following quantities in Eq. (6) can be approximated by using binomial expansions:

$$\begin{aligned} A &\approx r_0^2/4(1 - r_0^2/4) \\ B &\approx 1 - r_0^2/8 + r_0^4/32 \\ C &\approx r_0^2(1 - r_0^2) \\ D &\approx 1 - r_0^2/2 - r_0^4/8 \\ \mathcal{E}(s) &\approx \pi/2 \quad . \end{aligned} \tag{10}$$

By substituting the approximation shown in Eq. (10) into Eq. (6), the driving impedance, Eq. (5), for the antenna oriented perpendicular to the earth's magnetic field reduces to the following:

$$Z_{dp}^{\perp} = \frac{-j}{\pi\omega\epsilon_0(\kappa_{11}\kappa_{33})^{1/2}l}\left(ln\left\{\frac{2}{r_0\left[1 + (\kappa_{11}/\kappa_{33})^{1/2}\right]}\right\} - 1\right), \quad r_0 << 1 \quad . \tag{11}$$

A necessary check is to allow the earth's magnetic field $B_0 \rightarrow 0$; then $\kappa_{11} = \kappa_{33} = \kappa$, and $\kappa_{12} = 0$, which eliminates the anisotropy. Consequently, it is evident that Eqs. (5) and (11) reduce to the same formula giving the impedance of a center-fed cylindrical dipole in a

lossy, homogeneous, isotropic plasma:

$$Z_{dp} = \frac{-j}{\pi\omega\epsilon_0\kappa}\left[ln\left(\frac{l}{a}\right) - 1\right] \quad , \quad \frac{l}{a} >> 1 \quad . \tag{12}$$

Finally, if the electron and total ion densities $N \rightarrow 0$, then $\kappa \rightarrow 1$, and the impedance, Eq. (12), reduces to the purely capacitive reactance of a symmetrically driving dipole in free space:

$$Z_{dp} = \frac{-j}{\pi\omega\epsilon_0}\left[ln\left(\frac{l}{a}\right) - 1\right] \quad , \quad \frac{l}{a} >> 1 \quad . \tag{13}$$

2.3 Impedance Resonance for an Electron-Proton Plasma

The impedance of the electrically short antenna in free space has no resonances, since it is purely capacitive. However, the same antenna imbedded in an isotropic plasma will experience a resonance pole in the driving-point impedance, Eq. (12), at the plasma frequency; that is

$$\kappa = 1 - \sum_n X_n = 0 \tag{14}$$

and

$$f_p = \left(\sum_n f_{pn}^2\right)^{1/2} \quad . \tag{15}$$

There are additional resonances, which are caused by the anisotropy, in the form of zeros at the gyroresonances ($\kappa_{11} = \infty$) and additional poles at the hybrid resonances ($\kappa_{11} = 0$). To demonstrate the existence of the resonances, the plasma is first assumed to be lossless. The most general case having an algebraic solution is a plasma whose constituents are electrons and three different ion species. The additional complexity of the anisotropy contributes n zeros in the parallel impedance Eq. (8),

$$\lim_{\kappa_{11} \rightarrow \infty} |Z_{dp}^{\parallel}| \rightarrow 0 \tag{16}$$

and contributes n poles in the parallel impedance, Eq. (9),

$$\lim_{\kappa_{11} \rightarrow 0} |Z_{dp}^{\parallel}| \rightarrow \infty \quad . \tag{17}$$

The anisotropy also contributes n zeros in the perpendicular impedance, Eq. (11),

$$\lim_{\kappa_{11} \to \infty} |Z_{dp}^{\perp}| \to 0 \tag{18}$$

and contributes n poles,

$$\lim_{\kappa_{11} \to 0} |Z_{dp}^{\perp}| \to \infty \quad . \tag{19}$$

A comparison of Eq. (16) with Eq. (18) and Eq. (17) with Eq. (19) shows that the poles and zeros of the impedance occur at the zeros and poles, respectively, of κ_{11}. Consequently, the combination of signal frequency, types and densities of constituents, and magnetic field that gives the zeros and poles in κ_{11} gives the same poles and zeros, respectively, in the driving-point impedance for either orientation. Moreover, the impedance poles and zeros are independent of the antenna geometry, as long as $r_0 \ll 1$.

To illustrate the nature of the poles and zeros of the impedance for a plasma containing ions of finite mass, the case of a lossless anisotropic electron-proton plasma is presented in detail. For this case, the elements of the permittivity matrix, Eq. (3), become:

$$\kappa_{11} = 1 - \frac{X_e}{1 - Y_e^2} - \frac{X_1}{1 - Y_1^2} \tag{20a}$$

$$\kappa_{12} = \frac{X_e Y_e}{1 - Y_e^2} + \frac{X_1 Y_1}{1 - Y_1^2} \tag{20b}$$

$$\kappa_{33} = 1 - X_e - X_1 \quad , \tag{20c}$$

where the subscripts e and 1 refer to electron and proton, respectively. Using Eq. (4) in Eq. (20) and solving for the zeros in κ_{11} and κ_{33}, one obtains the following three frequencies: For κ_{11} zero,

$$\omega_{1,2} = \frac{1}{\sqrt{2}} \left\{ (\omega_{ue}^2 + \omega_{u1}^2) \pm \left[(\omega_{ue}^2 - \omega_{u1}^2)^2 + 4\omega_{pe}^2 \omega_{p1}^2 \right]^{1/2} \right\}^{1/2} \quad ; \qquad (21a)$$

for κ_{33} zero,

$$\omega_3 = \omega_{ue} \quad , \qquad (21b)$$

where

$$\omega_{ue} = (\omega_{pe}^2 + \omega_{ge}^2)^{1/2} \qquad (21c)$$

$$\omega_{u1} = (\omega_{p1}^2 + \omega_{g1}^2)^{1/2} \quad . \qquad (21d)$$

By using Eq. (21) in Eqs. (8) and (11), the pole and zero frequencies are determined directly. The poles of $Z_{dp}^{\perp}$ and $Z_{dp}^{\parallel}$ occur at the following frequencies:

$$\omega = \omega_u = \frac{\omega_{ue}}{\sqrt{2}} \left\{ \left[1 + \left(\frac{\omega_{u1}}{\omega_{ue}} \right)^2 \right] + \left[1 - \left(\frac{\omega_{u1}}{\omega_{ue}} \right)^2 + \left(\frac{2\omega_{pe}\omega_{p1}}{\omega_{ue}^2} \right)^2 \right] \right\}^{1/2} \qquad (22a)$$

$$\omega = \omega_{l1} = \frac{\omega_{ue}}{\sqrt{2}} \left\{ \left[1 + \left(\frac{\omega_{u1}}{\omega_{ue}} \right)^2 \right] - \left[1 - \left(\frac{\omega_{u1}}{\omega_{ue}} \right)^2 + \left(\frac{2\omega_{pe}\omega_{p1}}{\omega_{ue}^2} \right)^2 \right] \right\}^{1/2} \qquad (22b)$$

$$\omega = \omega_a = \left(\omega_{pe}^2 + \omega_{p1}^2 \right)^{1/2} \quad . \qquad (22c)$$

The zeros of $Z_{dp}^{\perp}$ and $Z_{dp}^{\parallel}$ occur at the following frequencies:

$$\omega = \omega_{ge} \qquad (23a)$$

$$\omega = \omega_{g1} \quad . \qquad (23b)$$

The five critical frequencies are positioned on an impedance diagram (Fig. 1) with frequency increasing to the right. The special conditions occurring at each of the frequencies are indicated at the top of the vertical lines above the frequencies. These lines separate the impedance into six regions, depending on the signal frequency used. The $\gtrless$ symbols used in the top four rows indicate that the parameter (on

PARAMETERS	REGIONS					
	1	2	3	4	5	6
	$K_{11} = \infty$	$\mu_{11} = 0$	$K_{11} = \infty$	$K_{33} = 0$	$K_{11} = 0$	
	$\mu_R^2 = \infty$	$\mu_X^2 = \infty$	$\mu_R^2 = \infty$	$\mu_0^2 = 0$	$\mu_X^2 = \infty$	
X_e	>	>	>	>	<	<1
Y_e	>	>	>	<	<	<1
X_1	>	< >	<	<	<	<1
Y_1	>	<	<	<	<	<1
K_{11}	+	−	+	−	−	+
K_{12}	−	−	−	+	+	+
K_{33}	−	−	−	−	+	+
μ_R^2	+	−	+	−	−	+
μ_L^2	−	−	−	−	+	+
μ_0^2	−	−	−	−	+	+
μ_X^2	−	−	−	−	+	+
	ω_{g1}	ω_{l1}	ω_{ge}	ω_a	ω_u	

RADIAN FREQUENCIES

FIG. 1 CRITICAL FREQUENCIES AND REGIONS IN THE DRIVING-POINT IMPEDANCE FOR A REPRESENTATIVE TWO-CONSTITUENT PLASMA

the left of each row) is greater or less than one. The ± symbols used in the bottom seven rows indicate that the parameter is greater or less than zero. Regardless of the particle density or the earth's magnetic field strength, the frequencies will always be ordered as indicated, with the exception that ω_a may be less than ω_{ge}.

The pole caused only by the electrons occurs at the upper hybrid frequency,[19] and the pole caused by the interaction of the electrons, ions, and anisotropy occurs at the lower hybrid frequency. The upper and lower hybrid frequencies for the impedance of an antenna in an anisotropic electron-proton plasma are shown in Fig. 2.

2.4 Impedance Resonances for a Multiple-Ion Plasma

The highest-order equation that can be solved algebraically is a fourth-order plasma containing electrons and three ionic constituents. It can be shown that the following biquadratic equation can be solved formally to give the four zeros in κ_{11} and the four poles in the impedance,

$$\omega^8 + P\omega^6 + Q\omega^4 + R\omega^2 + S = 0 \quad , \tag{24a}$$

where

$$P = \omega_{\mu e}^2 + \omega_{u1}^2 + \omega_{u2}^2 + \omega_{u3}^2 \tag{24b}$$

$$\begin{aligned} Q = {} & \{\omega_{pu}^2(\omega_{g1}^2 + \omega_{g2}^2 + \omega_{g3}^2) + \omega_{p1}^2(\omega_{pe}^2 + \omega_{g2}^2 + \omega_{g3}^2) \\ & + \omega_{p2}^2(\omega_{ge}^2 + \omega_{g1}^2 + \omega_{g3}^2) + \omega_{p3}^2(\omega_{ge}^2 + \omega_{g1}^2 + \omega_{g2}^2) \\ & + \omega_{g1}^2(\omega_{ge}^2 + \omega_{g3}^2) + \omega_{g2}^2\omega_{g3}^2\} \quad , \end{aligned} \tag{24c}$$

$$\begin{aligned} R = {} & \{\omega_{pu}^2[\omega_{g1}^2(\omega_{g2}^2 + \omega_{g3}^2) + \omega_{g2}^2\omega_{g3}^2] \\ & + \omega_{p1}^2[\omega_{g2}^2(\omega_{g2}^2 + \omega_{g3}^2) + \omega_{g2}^2\omega_{g3}^2] \\ & + \omega_{p2}^2[\omega_{pe}^2(\omega_{g1}^2 + \omega_{g3}^2) + \omega_{g1}^2\omega_{g3}^2] \\ & + \omega_{p3}^2[\omega_{pe}^2(\omega_{g1}^2 + \omega_{g2}^2) + \omega_{g1}^2\omega_{g2}^2] \\ & + \omega_{g1}^2\omega_{g2}^2\omega_{g3}^2\} \quad , \end{aligned} \tag{24d}$$

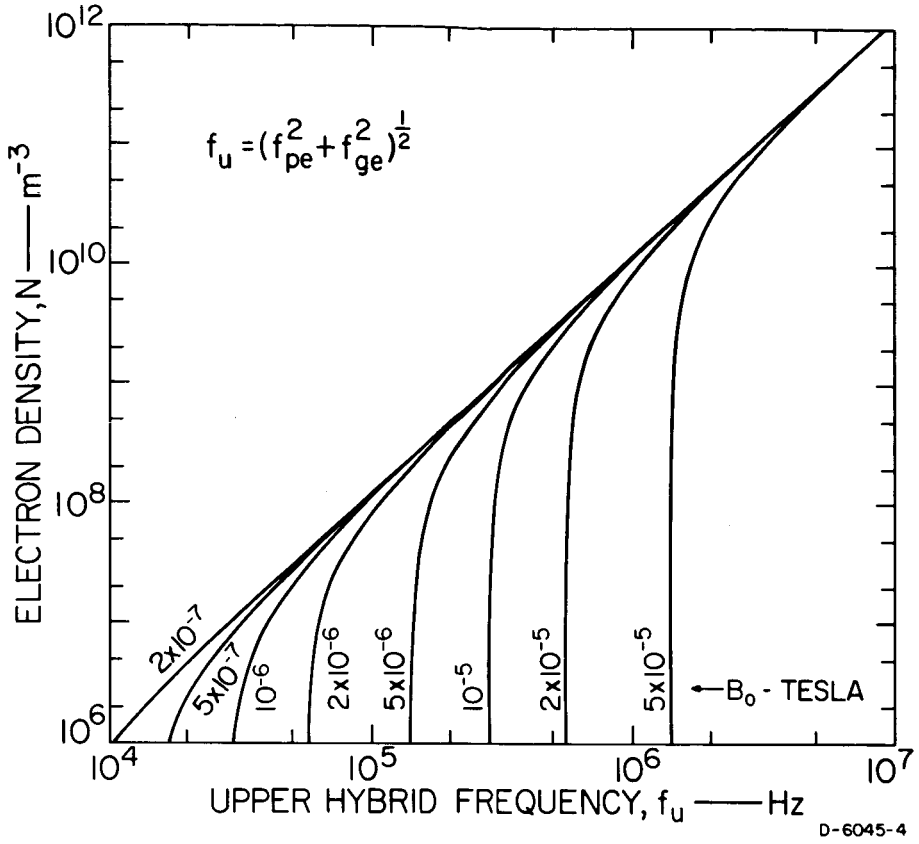

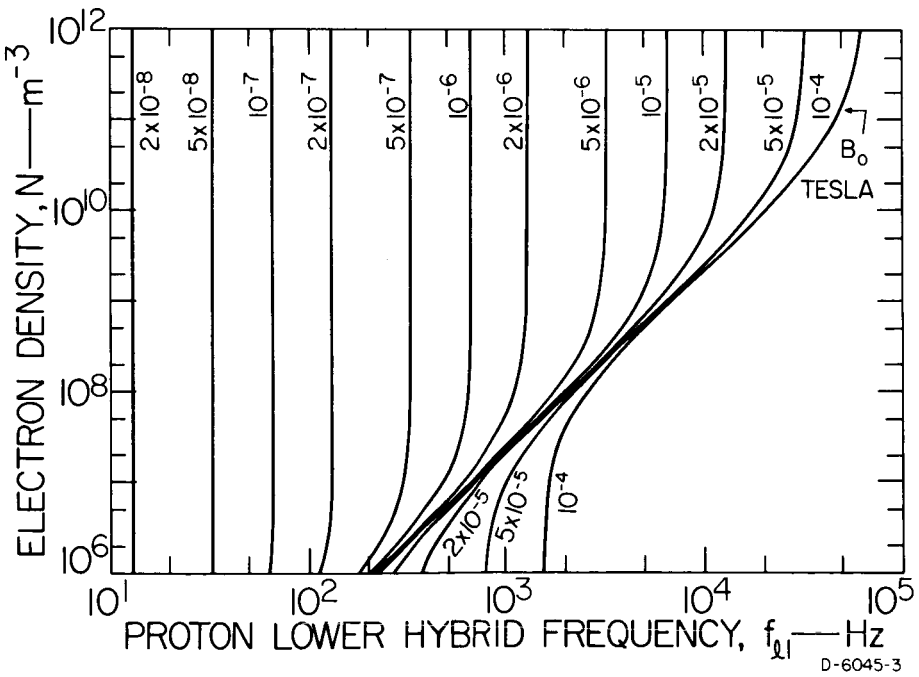

FIG. 2 THE UPPER-HYBRID FREQUENCY, f_{ue}, AND LOWER-HYBRID FREQUENCY, $f_{\ell 1}$, FOR AN ELECTRON-PROTON PLASMA

$$S = \{\omega_{pe}^2\omega_{g1}^2\omega_{g2}^2\omega_{g3}^2 + \omega_{p1}^2\omega_{ge}^2\omega_{g2}^2\omega_{g3}^2 + \omega_{p2}^2\omega_{ge}^2\omega_{g1}^2\omega_{g2}^2 + \omega_{p3}^2\omega_{ge}^2\omega_{g1}^2\omega_{g2}^2 + \omega_{ge}^2\omega_{g1}^2\omega_{g2}^2\omega_{g3}^2\} \quad . \tag{24e}$$

The subscripts 1, 2, and 3 refer to the ions in order of increasing mass. The fifth impedance pole is determined from the zero in κ_{33}, which occurs at the following frequency:

$$\omega = (\omega_{pe}^2 + \omega_{p1}^2 + \omega_{p2}^2 + \omega_{p3}^2)^{1/2} \quad . \tag{25}$$

The four impedance zeros are determined from the poles in κ_{11} and occur at the gyrofrequencies of the four constituents.

For multiple-ionic plasmas of more than four constituents, one must employ the usual empirical or numerical methods to determine the anisotropically generated impedance poles by calculating the zeros in κ_{11} and the zero in κ_{33}. However, the ordering of the f_{ln}, f_{gn} pair for each of the ions is the same as that shown for the proton in Fig. 1. Since the $(n + 1)$th ion is heavier than the nth, the frequency pair $f_{l(n+1)}$, $f_{g(n+1)}$ is always lower than the f_{ln}, f_{gn} pair. The region of $f_{gn} \leq f \leq f_{ln}$ is described by the same characteristics of κ_{11}, κ_{33}, and impedance as in the case of the proton region of $f_{g1} \leq f \leq f_{l1}$.

2.5 Effect of Collisions on the Impedance Resonances

The discussion in Secs. 2.2 and 2.3 has been idealized to the case of a lossless ionosphere. As in the case of any passive L-C network containing poles, the main effect of introducing losses (particle collisions) is to reduce the value of the impedance at the poles from infinite to finite. The secondary effect is to shift slightly the position of the poles and zeros. In order to examine the effects of collisions, the representative case of electron collisions is examined. By using Eq. (3d, a, and c), expand as follows:

$$\kappa_{11} = 1 - X_e \frac{(1 + Z_e^2 - Y_e^2) - jZ_e(1 + Z_e^2 + Y_e^2)}{(1 - Z_e^2 - Y_e^2)^2 + 4Z_e^2} \tag{26a}$$

$$\kappa_{33} = 1 - X_e(1 - jZ_e) \quad . \tag{26b}$$

Examination of Eq. (26a) reveals that $|\kappa_{11}|$, $\mathrm{Re}(\kappa_{11})$, and $\mathrm{Im}(\kappa_{11})$ are all maximized at the following frequency:

$$\omega_c = (\omega_{ge}^2 + \nu_e^2)^{1/2} \quad . \tag{27}$$

The maximum values at this peak frequency are approximated by

$$\mathrm{Re}(\kappa_{11}) \approx X_e Y_e^2 / 4Z_e^2 \quad , \quad \omega = \omega_c \tag{28a}$$

$$\mathrm{Im}(\kappa_{11}) \approx X_e / 2Z_e \quad , \quad \omega = \omega_c \quad . \tag{28b}$$

3. IMPEDANCE PLOTS AND DISCUSSION

The significant features of the poles and zeros of the driving-point impedance are demonstrated in the following figures. The series real (resistive) and imaginary (reactive) components of the parallel [Eq. (1)] and perpendicular [Eq. (11)] impedances are plotted as a function of frequency for various combinations of geophysical and antenna parameters. The antenna length and radius are chosen to ensure that the antenna is an electrically short dipole under all typical ionospheric circumstances for frequencies below 100 kHz. The $l/a = 10^3$ with l = 1m and a = 0.001m was used in all but one case, in which $l/a = 10^2$ with l = 1m and $a = 10^{-2}$m. The cases are presented in order of decreasing height—that is, of increasing plasma complexity.

The simplest realistic macroscopic plasma model of the ionosphere[20] is one for the magnetosphere which is essentially a weakly anisotropic protonosphere. Consequently, the impedance in Fig. 3 shows peaks at f_u, f_a, and f_{l1}. Since $f_{ge} \ll f_{pe}$, the upper hybrid resonance in κ_{11} is $f_u \approx f_{pe}$; and since the proton plasma frequency $f_{p1} \ll f_{pe}$, the resonance in κ_{33} is $f_a \approx f_{pe}$. Thus two peaks in the impedance occur at approximately f_{pe}. The third peak occurs at the lower hybrid resonance in κ_{11} and is $f_{l1} \approx f_{pe}(m_e/m)^{1/2}$, which is independent of the earth's magnetic field.

For the region $f > f_{pe}$, the impedance is capacitive with a small resistive component. The capacitance increases with increasing frequency from f_{pe} and eventually approaches the capacitance of the antenna in free space. The resistance in this region is caused exclusively by the ionospheric losses and would theoretically be zero if collisions were neglected. For the two regions $f_{ge} < f < f_{pe}$ and $f < f_{l1}$, the impedance is inductive with a small resistive component. The reactance becomes inductive because the signal frequency is in the "cutoff" region of the ionosphere, as indicated by the fact that κ_{11} and κ_{33} have negative real parts (see Fig. 1). The inductance is approximately constant for frequencies not near the resonances; consequently, the inductive reactance increases proportionally with frequency. Again, the resistance in these regions is caused by ionospheric losses and would be zero if collisions were neglected.

For the region $f_{l1} < f < f_{ge}$, the impedance is resistive with a small capacitive reactance. The large resistance is caused by the fact that κ_{11} is positive and κ_{33} is negative; consequently, the resistance represents primarily radiation losses in the ionosphere and would not change appreciably even if ionospheric collisions were neglected. Although this is a quasi-static analysis, there is a quasi-static component of both the electric field and the magnetic field in time and space quadrature[4] such that radiation can exist in the quasi-static zone of the antenna. The capacitive reactance is unusual in that it is $\sim f^{+1}$; that is, the capacitance is actually $\sim f^{-2}$ because of the interaction of the dipole with the ionosphere. Thus the reactive element in this region is effectively a negative inductance.

The impedance in Fig. 4 is plotted for the identical magnetospheric model used for Fig. 3. However, in Fig. 4, a wider antenna is used, with the half length, l = 1m and the radius, $a = 10^{-2}$m, so that the ratio $l/a = 10^2$. The impedance in Fig. 4 is reduced in magnitude by less than 50 percent everywhere, although the radius was increased by a factor of 10. Because the radius appears only in the ln term in Eq. (11), large changes in a result in only small changes in impedance. On the other hand, if a thinner antenna were used, for example, l = 10m, $a = 10^{-3}$m, so that $l/a = 10^4$, the impedance would be reduced almost an order of magnitude from that in Fig. 3. In fact, if the ratio l/a is preserved, the impedance scales $\sim l^{-1}$; for example, with l = 10m, and $a = 10^{-2}$m, so that $l/a = 10^3$, the impedance would be reduced exactly one order of magnitude from that in Fig. 3.

It is noteworthy that the resonant frequencies are not shifted by any of the four cases of changing l, a, or l/a discussed above. A comparison of Figs. 3 and 4 demonstrates this point for the first two cases above.

The effect of the increase by 10^2 in the collision rate to $\nu_e = 1\ \mathrm{sec}^{-1}$ was investigated. The increased ν_e produced only minor changes in the impedance, because, in spite of the increased ν_e, the inequality $X_e >> Y_e^2 >> Z_e$ remained unchanged. Although it is not demonstrated in the graphs, the main effect is to decrease the magnitude of the reactance and to increase the resistance near the resonances. This effect is essentially the same for all the four combinations of l, a, and l/a discussed previously.

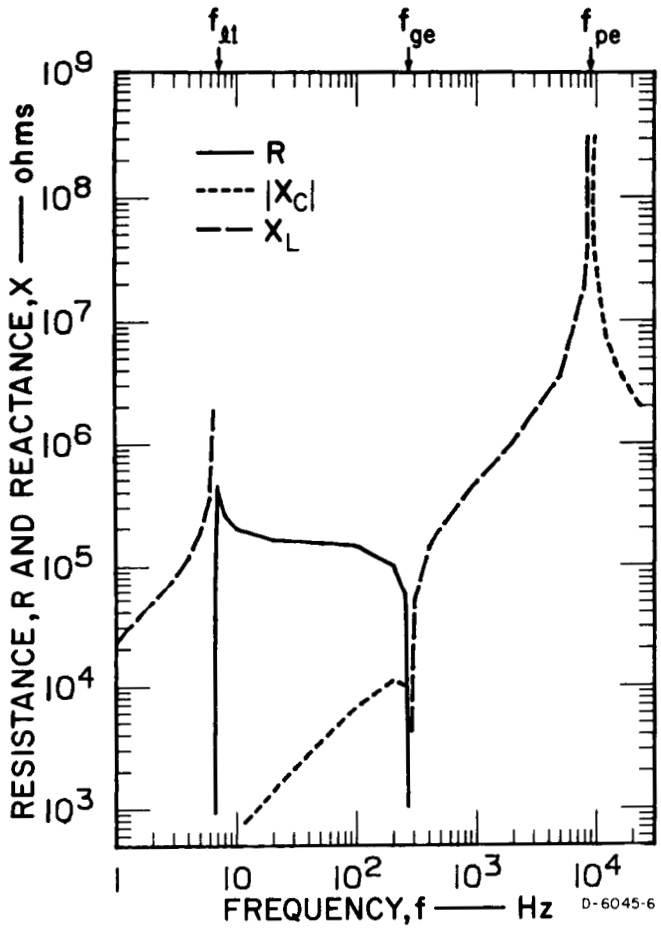

FIG. 3 VARIATION OF DRIVING-POINT IMPEDANCE WITH FREQUENCY FOR PERPENDICULAR ORIENTATION FOR ℓ = 1m; a = 10^{-3}m; AND $N_e = N_i = 10^6 m^{-3}$, $\nu_e = 10^{-2} sec^{-1}$, AND $B_o = 10^{-8}$ tesla, FOR $R \approx 10R_E$

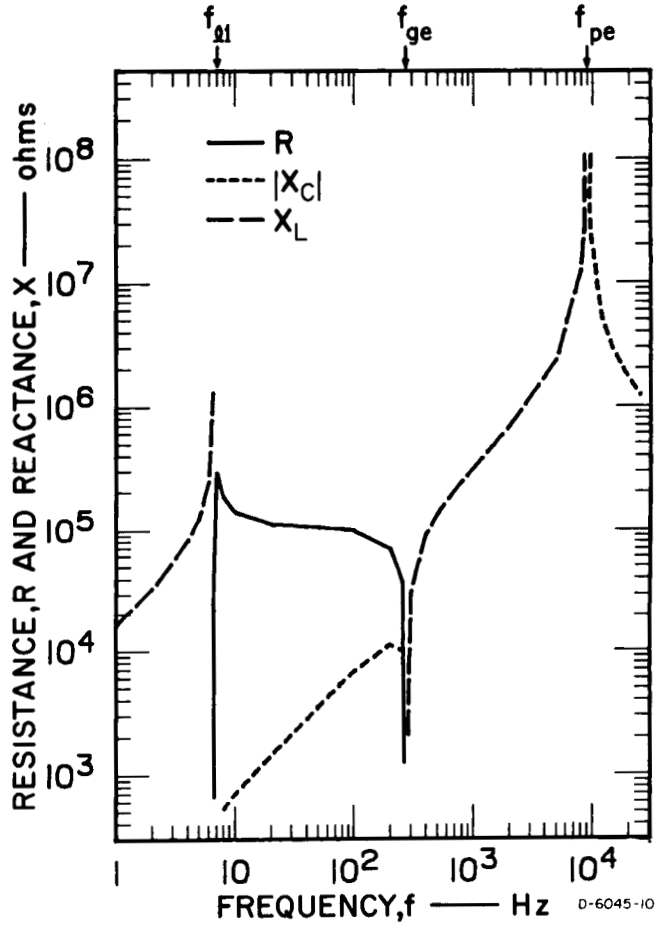

FIG. 4 VARIATION OF DRIVING-POINT IMPEDANCE WITH FREQUENCY FOR PERPENDICULAR ORIENTATION FOR ℓ = 1m; a = 10^{-2}m; AND $N_e = N_i = 10^6 m^{-3}$, $\nu_e = 10^{-2} sec^{-1}$, AND $B_o = 10^{-8}$ tesla, FOR $R \approx 10R_E$

In Fig. 5, the impedance is shown for the same antenna with perpendicular orientation as in Fig. 3, but in this case the plasma parameters have been changed to those typical for a distance of about two earth radii. The general structure of the impedance curves is the same in both figures, with the exception that the resonant frequencies are increased by at least 10^2. The slope and sign of the reactance as well as the ratio of reactance to resistance in each of the frequency regions is essentially the same as in Fig. 3. The magnitudes of the reactances are about half those in Fig. 3.

In Fig. 6, the impedance is shown for the same antenna and plasma parameters as in Fig. 5, but in this case the antenna is oriented parallel to the earth's magnetic field. The reactance shows the identical poles at $f_u \approx f_{pe}$ and f_{l1}, but there is no pole at $f_a \approx f_{pe}$, since κ_{33} does not appear in the coefficient in the $Z^{\parallel}_{dp}$ in Eq. (8). There reactance also shows the identical zeros at f_{ge}. The reactance and resistance are about the same in Figs. 5 and 6 for $f > f_{ge}$. However, for $f_{l1} < f < f_{ge}$ in Fig. 6, both the capacitive reactance and the resistance vary approximately as f^{-1}; consequently, the capacitance is constant in frequency. The magnitude of the capacitive reactance is about twice the resistance and is much larger than in Fig. 5. For $f < f_{l1}$, the impedance is inductive with a small resistive component and is about ten times that in Fig. 5.

In Fig. 7, the antenna and its orientation are again the same as in Fig. 3, but in this case the plasma parameters have been changed to those typical for a height of around 1000 km. This ionospheric model is a three-constituent plasma composed of H^+ and O^+ ions as well as electrons, and it is the most complex plasma model considered. There are reactance poles at $f_u \approx f_{pe}$, $f_a \approx f_{pe}$, f_{l1}, and f_{l2}. Since there are two ions in this case, there are two lower hybrid frequencies: f_{l1} caused by the H^+ ion density and f_{l2} caused by O^+ ion density. For the multiple-ion case, each of the lower hybrid frequencies is affected by the presence of the other ions. That is, if each of the constituents were present alone (at density N_e, N_1, or N_2), each of the single-ion lower hybrid frequencies would be different from f_{l1} or f_{l2}. The shifting of the lower hybrid frequencies by the addition of another constituent (as long as the electron and ion densities are readjusted to maintain a neutral plasma) can be seen in Eq. (24). One interesting peculiarity is that the reactance does not change sign at f_a; this occurs only in the case of $f_{ge} < f_a \approx f_{pe}$. There are reactance zeros at f_{ge}, f_{g1}, and f_{g2}, one for each constituent.

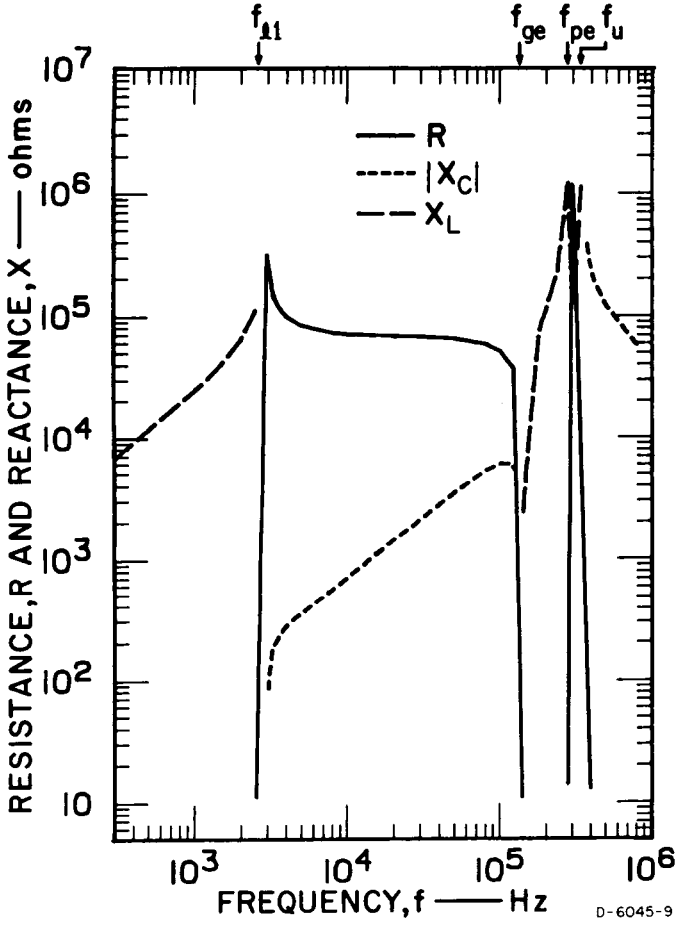

FIG. 5 VARIATION OF DRIVING-POINT IMPEDANCE WITH FREQUENCY FOR PERPENDICULAR ORIENTATION FOR ℓ = 1m, a = 10^{-3}m, $N_e = N_1 = 10^9 m^{-3}$, $\nu_e = 10^{-1} sec^{-1}$, AND $B_o = 5 \times 10^{-6}$ tesla, FOR R ≈ $2R_E$

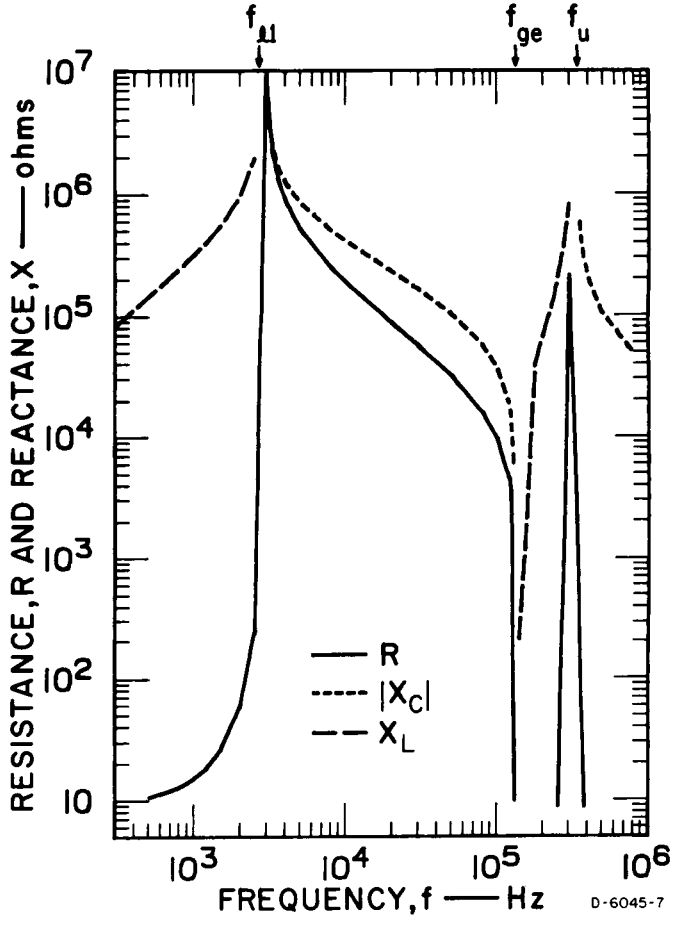

FIG. 6 VARIATION OF DRIVING-POINT IMPEDANCE WITH FREQUENCY FOR PARALLEL ORIENTATION FOR ℓ = 1m; a = 10^{-3}m; AND $N_e = N_1 = 10^9 m^{-3}$, $\nu_e = 10^{-1} sec^{-1}$, AND $B_o = 5 \times 10^{-6}$ tesla, FOR R ≈ $2R_E$

In Fig. 8, the impedance is shown for the same antenna and orientation as in Fig. 3, but in this case the plasma parameters have been changed to those typical for a height of about 300 km. This is an ionospheric model for a maximum electron and O^+ ion density. There are reactance poles at $f_u (\approx f_{pe})$ and f_{l2}. There are reactance zeros at f_{ge} and f_{g2} (the critical frequencies f_{p1} and f_{g1} are zero in this case, since N_1 of H^+ ion is assumed to be negligible). The structure of the impedance in Fig. 8 for $f > f_{g2}$ is similar to that in Fig. 3 for $f > 1$ Hz, including the same frequency regions with the same reactance sign and slope. The most significant difference is that the critical frequencies f_{pe}, f_{ge}, and f_{l1} in Fig. 8 are larger by more than 10^2 than f_{pe}, f_{ge}, and f_{l2} in Fig. 3. The frequency region $f < f_{g2}$ in Fig. 8 is similar to the region $f_{l2} < f < f_{ge}$: Both regions are resistance with a small capacitive reactance. The impedance magnitude is the smallest of all the cases considered, because the electron density is the largest of all the cases.

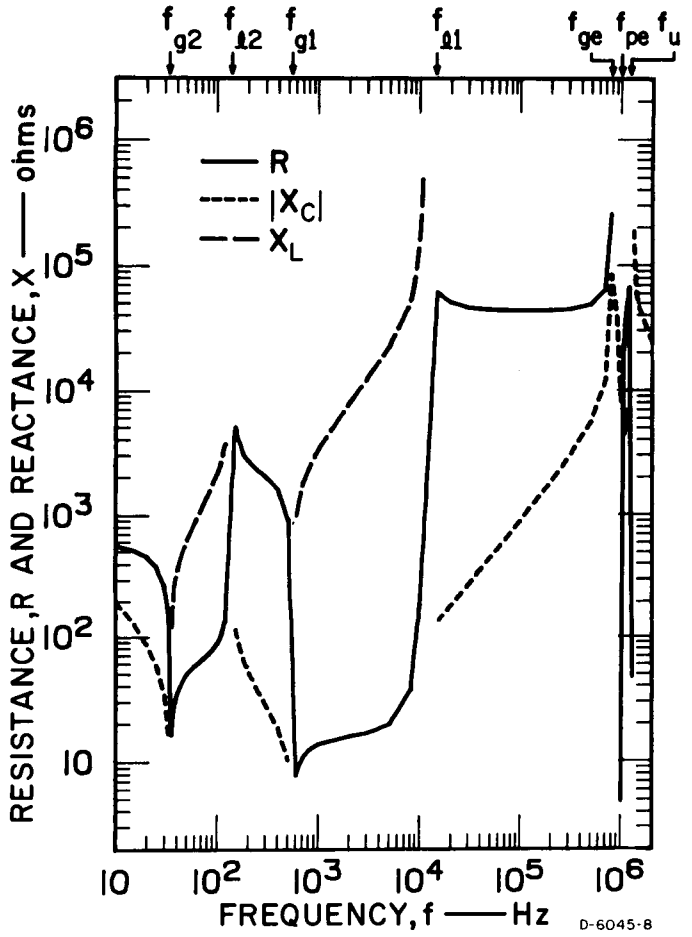

FIG. 7 VARIATION OF DRIVING-POINT IMPEDANCE WITH FREQUENCY FOR PERPENDICULAR ORIENTATION FOR ℓ = 1m; a = 10^{-3}m; AND $N_e = 8 \times 10^9 m^{-3}$, $N_1 = N_2 = 4 \times 10^9 m^{-3}$, $\nu_e = 50\ sec^{-1}$, $\nu_1 = 1\ sec^{-1}$, $\nu_2 = 2.5 \times 10^{-1}\ sec^{-1}$, AND $B_o = 3.6 \times 10^{-5}$ tesla, FOR h ≈ 1000 km

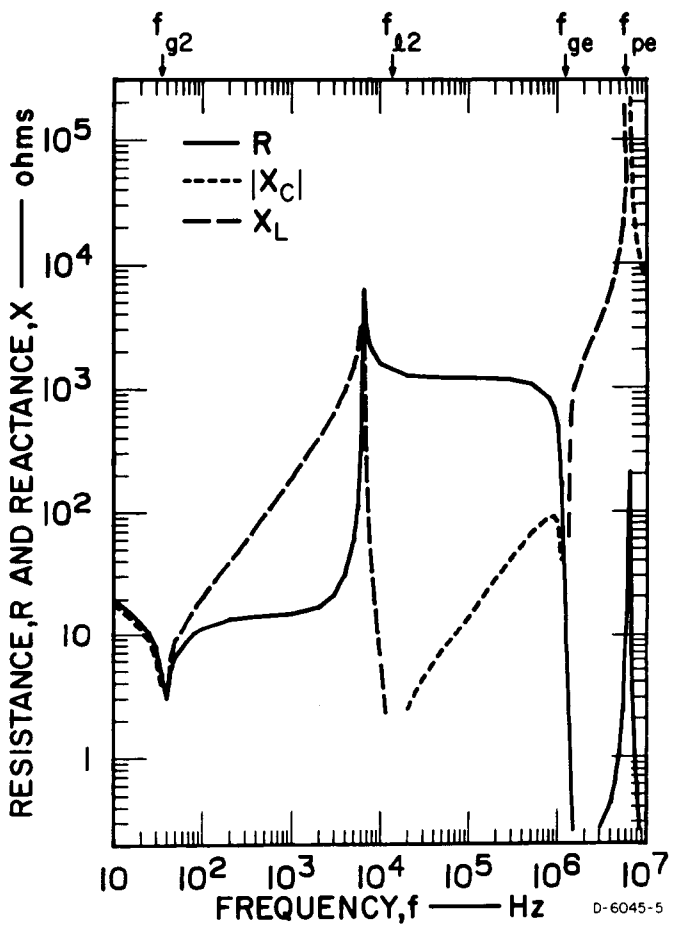

FIG. 8 VARIATION OF DRIVING-POINT IMPEDANCE WITH FREQUENCY FOR PERPENDICULAR ORIENTATION FOR ℓ = 1m; a = 10^{-3}m; AND $N_e = N_2 = 5 \times 10^{11} m^{-3}$, $\nu_e = 10^3 sec^{-1}$, $\nu_2 = 1\ sec^{-1}$, AND $B_o = 4 \times 10^{-5}$ tesla, FOR h ≈ 300 km

4. CONCLUSIONS

The six figures discussed in Chap. 3 demonstrate the variations of the driving-point impedance for six typical antenna and ionospheric plasma models. Figures 3 and 4 show that the critical frequencies (reactive poles and zeros) in the impedance are independent of changes of antenna length or radius or both. The impedance varies with radius as $(-ln\ a)$ and with length as $(ln\ l)/l$; consequently, the impedance is much more sensitive to changes in length than in radius.

Figures 5 and 6 show that the critical frequencies are independent of the parallel or perpendicular orientation of the antenna, with the exception that f_a does not appear in the $Z_{dp}^{\parallel}$. In most cases, $f_{ge} \ll f_{pe}$ so $f_a \approx f_u \approx f_{pe}$; consequently, the f_a cannot be distinguished from the f_u.

Figures 3, 5, 7, and 8 give the impedances for antennas with the same size, shape, and perpendicular orientation but with different ionospheric parameters. A comparison of these figures shows that the basic structure of the impedance, including the reactance sign and the slope, is the same for the various frequency regions considered. The significant difference among these figures is that the value of the critical frequencies tends to increase with decreasing height, that is, with increasing constituent densities and the earth's magnetic field strength. The reactance poles [gyroresonances, that is, zeros in κ_{11}; see Eq. (3a)] are determined exclusively by the earth's field and constituent masses. The reactance zeros (hybrid resonances, that is, poles in κ_{11}) are determined by the earth's field and the constituent masses and densities.

The location of the critical frequencies in the impedance can be used in the following manner to diagnose the ionosphere:

(1) The highest (in frequency) pole is the electron gyroresonance and is used to determine the earth's magnetic field, B_o.

(2) The remaining poles are used to determine the masses of the ions, the lower (in frequency) the pole the larger the mass.

(3) The highest zero is the upper (electron) hybrid resonance; since B_o is known already from (1) above, the electron density, N_e, is determined.

(4) The second highest zero is the lower hybrid resonance of the lightest ion and is dependent mainly on this ion density N_1, mass m_1, and B_o. Since m_1 and B_o are known from (1) and (2) above, respectively, the N_1 is determined.

(5) The next highest zero is the lower hybrid resonance of the second lighest ion and is dependent mainly on this ion density N_2 and mass m_2, as well as on N_1, m_1, and B_o. Since B_o, N_1, m_1, and m_2 are known from (1), (2), and (3) above, the N_2 is determined. The density of each succeeding ion is determined in a similar manner, making use of the densities and masses of the light ions as well as of the B_o.

Summarizing, the frequency location of the reactance poles and zeros in the impedance curves can be used diagnostically to determine the earth's magnetic field strength, electron density, and ion masses and densities. These resonances are independent of the antenna size and independent of the electron and ion collision rates to the first-order approximation.

If the known antenna were imbedded into a known homogeneous ionosphere (uniquely determined by the reactance resonances), the impedance values between the resonances theoretically could be used to verify the antenna geometry and the ionospheric parameters. However, if these impedance values deviated from the theory, it should be possible to obtain additional information. For example, if the antenna effective length were larger than the physical length (often the case for dipoles imbedded in plasmas), the impedance values would be a fixed percentage lower everywhere. Increased electron temperatures, hence increased collision rates, would give disproportionately high resistance. The presence of an ion sheath isolating the antenna from the neutral homogeneous ionosphere would increase the capacitive reactance and reduce the inductive reactance.

REFERENCES

1. W. S. Ament, J. C. Katzin, M. Katzin, and B.Y.-C. Koo, "Impedance of a Cylindrical Dipole Having a Sinusoidal Current Distribution in a Homogeneous Anisotropic Ionosphere," *Radio Sci. J. Res. NBS,* Vol 68D, No. 4, pp. 379-406 (1964).

2. W. E. Blair, "On the Driving-Point Impedance of a Short Cylindrical Antenna in the Anisotropic Ionosphere," paper presented at 1963 Fall URSI Meeting, Washington, D.C.

3. W. E. Blair, "The Driving-Point Impedance of an Electrically Short Cylindrical Antenna in the Ionosphere," Tech Rept. EE-109, Electrical Engineering Department, University of New Mexico, Albuquerque, N.M. (1964).

4. K. G. Balmain, "The Impedance of a Short Dipole Antenna in a Magnetoplasma," *IEEE Trans.*, Vol. AP-12, No. 5, pp. 605-617 (1964).

5. P. A. Sturrock, "Dipole Resonances in a Homogeneous Plasma in a Magnetic Field," *Phys. Fluids*, Vol. 8 No. 1, pp. 88-96 (1965).

6. K. D. Baker, A. M. Despain, and J. C. Ulwick, "Simultaneous Comparison of RF Probe Techniques for Determination of Ionospheric Electron Density," *J. Geophys. Res.*, Vol. 71, No. 3, pp. 935-944 (1960).

7. J. A. Fejer, "Excitation of the Lower Hybrid Resonance by an Antenna in the Ionosphere," *Radio Sci.* Vol. 1 (New Series), No. 8 pp. 447-456 (1966).

8. W. S. Ament, M. Katzin, J. R. McLaughlin, and W. W. Zachary, "Satellite Antenna Radiation Properties at VLF in the Ionosphere," Report No. ONR-4250-1, Electromagnetic Research Corporation, College Park, Md. (1965).

9. K. R. Cook and B. C. Edgar, "Current Distribution and Impedance of a Cylindrical Antenna in an Isotropic Compressible Plasma," *Radio Sci.*, Vol. 1 (New Series), No. 1, pp. 13-19 (1966).

10. H. Staras, "The Impedance of an Electric Dipole in a Magneto-Ionic Medium," *IEEE Trans.* Vol. AP-12, No. 6, pp. 695-702 (1964).

11. D. A. deWolf, "Impedance of a Small VLF Dipole in the Ionosphere," *Radio Sci.*, Vol. 1 (New Series), No. 5, pp. 571-575 (1966).

12. H. H. Kuehl, "Resistance of a Short Antenna in a Warm Plasma," *Radio Sci.* Vol. 1 (New Series), No. 8, pp. 971-976 (1966).

13. H. H. Kuehl, "Computations of the Resistance of a Short Antenna in a Warm Plasma," *Radio Sci.*, Vol. 2 (New Series), No. 1, pp. 73-76 (1967).

14. K. G. Balmain, "Impedance of a Short Dipole in a Compressible Plasma." *Radio Sci. J. Res. NBS,* Vol. 69D, No. 4, pp. 549-556 (1965).

15. J. Galejs, "Impedance of a Finite Insulated Cylindrical Antenna in a Cold Plasma with a Long Magnetic Field," *IEEE Trans.*, Vol. AP-14, No. 6, pp. 727-736 (1966).

16. J. Galejs, "Impedance of a Finite Insulated Antenna in a Cold Plasma with a Perpendicular Magnetic Field," *IEEE Trans.*, Vol. AP-15, No. 6, pp. 737-748 (1966).

17. K. G. Budden (1961), *Radio Waves in the Ionosphere* (Cambridge University Press, Cambridge, England 1961).

18. C. L. Chen and S. R. Seshadri, "Infinite Insulated Cylindrical Antenna in a Simple Anisotropic Medium," *IEEE Trans.* Vol. AP-14, No. 6, pp. 715-726 (1966).

19. T. H. Stix, *The Theory of Plasma Waves* (McGraw-Hill Book Company, Inc., New York, N.Y., 1962).

20. F. S. Johnson, *Satellite Environment Handbook*, (second edition, Stanford University Press, Stanford, California, 1965).